EFFICIENT MODELING OF POLARIZED REFLECTION SPECTRA IN METASURFACES USING DEEP LEARNING FRAMEWORKS

Alexandra Ilie[1], Doina Mănăilă-Maximean[2,3], Octavian Dănilă[4]

Modeling the electromagnetic responses of metasurfaces, advanced materials engineered to manipulate electromagnetic waves, remains computationally intensive, particularly for complex geometries such as polygonal and ring-like designs. This study explores the potential of frequency-domain prediction, followed by spectral transformation, as a viable approach for capturing x- and y-polarized reflection spectra of metasurfaces. To this end, a deep learning framework is developed, combining Variational Autoencoders (VAEs) and Convolutional Neural Networks (CNNs). The VAE effectively encodes spectral features in a low-dimensional latent space, while the CNN utilizes residual connections to directly map metasurface patterns to their spectral responses. By integrating frequency-domain representations with inverse Fourier transforms, the framework ensures compatibility with traditional time-domain data while maintaining computational efficiency. The proposed models achieve high predictive accuracy, with the VAE outperforming the CNN across multiple error metrics. This dual focus on methodological development and performance evaluation demonstrates the feasibility and advantages of integrating machine learning for rapid and precise metasurface analysis and design.

Keywords: Metasurfaces, Deep Learning, Variational Autoencoders, Convolutional Neural Networks, Electromagnetic Response Prediction

1. Introduction

Metasurfaces are advanced engineered materials designed to manipulate electromagnetic waves [1] [2] [3] with exceptional precision. These materials have revolutionized various fields, including wireless communications [4], [5], [6], imaging technologies [7], [8], [9], and sensing systems [10], [11], [12] [13] [14]. Despite their potential, accurately modeling and predicting the electromagnetic responses of metasurfaces poses significant computational challenges. Traditional simulation

[1] Faculty of Engineering in Foreign Languages, National University of Science and Technology POLITEHNICA of Bucharest, Romania

[2] Prof., Dept. of Physics, National University of Science and Technology POLITEHNICA of Bucharest, Romania

[3] Academy of Romanian Scientists, Romania, e-mail: doina.manaila@upb.ro

[4] Associate Professor, Faculty of Applied Sciences, National University of Science and Technology POLITEHNICA of Bucharest, Romania, Corresponding Author: danila.octavian@upb.ro

techniques, such as finite-difference time-domain (FDTD) methods [15], [16], are computationally intensive, particularly when dealing with intricate geometrical designs like PLG (Polygonal) and PLR (Polygonal Ring) metasurfaces, which feature concentric polygonal arrangements. As the complexity of these metasurface geometries increases, scalability and efficiency bottlenecks emerge, limiting the practical application of traditional simulation methods. To address these limitations, we propose a predictive modeling approach that efficiently captures the complex response patterns of metasurfaces while significantly reducing computational overhead. Unlike conventional time-domain simulations that solve Maxwell's equations iteratively, our method operates in the frequency domain. Specifically, given an input metasurface design $\mathbf{D}$, we predict its frequency-domain response $\mathbf{R}(\omega)$, which consists of the x- and y-polarization components:

$$\mathbf{R}(\omega) = \begin{bmatrix} R_x(\omega) \\ R_y(\omega) \end{bmatrix}$$

Here, $R_x(\omega)$ and $R_y(\omega)$ denote the reflection spectra for x- and y-polarizations as functions of frequency ω. By leveraging spectral characteristics, such as resonance peaks, our predictive model eliminates the need for iterative field calculations.

To convert the frequency-domain data back to the time domain, we employ the inverse Fourier transform:

$$\mathbf{S}(t) = \mathcal{F}^{-1}[\mathbf{R}(\omega)] = \int_{-\infty}^{\infty} \mathbf{R}(\omega) e^{j\omega t} \, d\omega$$

This transformation ensures compatibility with traditional simulation outputs while maintaining computational efficiency. Our framework leverages state-of-the-art deep learning models, including Variational Autoencoders (VAEs) and Convolutional Neural Networks (CNNs), which are trained to minimize prediction errors through metrics like Mean Squared Error (MSE) and Mean Absolute Error (MAE).

A Variational Autoencoder (VAE) is a type of deep generative model that combines variational Bayesian principles with autoencoder architectures. It comprises an encoder that maps input data into a latent space represented by a probability distribution, and a decoder that reconstructs data samples from this latent representation. This probabilistic design enables VAEs to model data distributions and generate realistic samples resembling the original dataset [17].

Convolutional Neural Networks (CNNs), on the other hand, are a class of deep learning models well-suited for processing structured data, such as images. CNNs utilize convolutional layers to apply filters to local regions of the input, effectively capturing spatial hierarchies and patterns. This ability to extract meaningful features makes CNNs particularly powerful for tasks involving complex visual or structural data [18].

By shifting focus to the frequency domain, this modeling strategy enhances the ability to capture intricate spectral features that are difficult to resolve in the time domain [19]. The resulting predictive framework streamlines the metasurface design process, enabling real-time predictions and rapid optimization. This capability

is essential for advancing metasurface applications in high-performance technologies, where speed and precision are critical.

2. Methodology

2.1 Dataset Description

The dataset utilized in this study comprises binary metasurface patterns encoded as 16×16 matrices. Each matrix element represents the presence (1) or absence (0) of a square copper patch ($0.5\,\text{mm} \times 0.5\,\text{mm} \times 0.018\,\text{mm}$) on a dielectric substrate. The substrate material is characterized by a permittivity of $\varepsilon_r = 2.65 \times (1 + 0.003i)$ and a permeability of $\mu_r = 1$, backed by a 0.18 mm-thick copper plate. A 1-mm padding surrounds the unit cell, providing periodic boundary conditions in the x- and y-directions and open boundaries in the z-direction.

Electromagnetic (EM) responses for these patterns were calculated using finite element methods (FEM) in CST Studio Suite. An x-polarized plane wave was normally incident on the metasurface, and the reflected spectra were computed for x-polarized (R_x) and y-polarized (R_y) components over a frequency range of 2 GHz to 12 GHz, sampled at 1001 points. The spectral data effectively captures the metasurface's key resonance and reflection behaviors [20]

For this study, the dataset was divided into two primary classes of metasurface geometries: the Polygonal (PLG) class, characterized by solid and connected polygonal shapes, and the Polygonal Ring (PLR) class, which consists of concentric polygonal patterns resembling rings. To optimize the learning process, the EM responses were transformed into the frequency domain using a real Fast Fourier Transform (FFT). This preprocessing step enhances the models' ability to capture meaningful spectral features, such as resonance peaks, while reducing computational complexity.

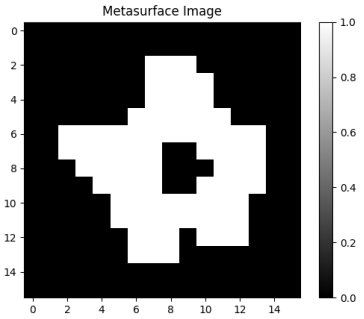

(A) Metasurface image for a sample pattern.

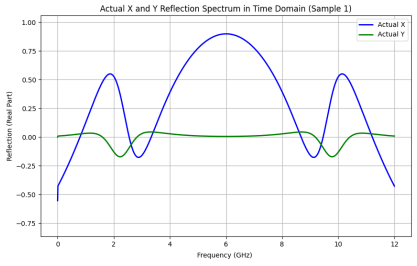

(B) Actual x and y reflection spectra in the time domain.

FIGURE 1. Metasurface dataset visualization. (A) Binary metasurface pattern and (B) corresponding time-domain reflection spectra.

2.2 Model Architectures

Two deep learning models were developed to predict the frequency-domain reflection spectra of metasurfaces: a Variational Autoencoder (VAE) and a Convolutional Neural Network (CNN) with residual connections. Each model was tailored to exploit the spectral characteristics of metasurface responses, enabling efficient prediction.

2.2.1 Variational Autoencoder (VAE)

The VAE is a deep generative model designed to encode metasurface patterns into a low-dimensional latent space while retaining sufficient information for accurate reconstruction. The VAE architecture comprises three core components: an encoder, a reparameterization layer, and a decoder.

The encoder consists of three 1D convolutional layers, each followed by Rectified Linear Unit (ReLU) activations [21] and dropout layers [22] to prevent overfitting. These layers reduce the input data to a compact latent representation by computing the mean (μ) and log variance ($\log \sigma^2$) of a Gaussian distribution. The reparameterization layer samples latent variables (z) from this distribution using:

$$z = \mu + \varepsilon \cdot \sigma, \quad \varepsilon \sim \mathcal{N}(0, I),$$

ensuring differentiability for gradient-based optimization.

The decoder reconstructs the reflection spectra from z using a fully connected layer followed by three transposed convolutional layers. The output layer ensures that the reconstructed spectra have the same dimensions as the target (2×501).

To optimize the VAE, the loss function combines reconstruction loss, measured by Mean Squared Error (MSE), and a Kullback-Leibler (KL) divergence term [17] that regularizes the latent space:

$$\mathcal{L}_{\text{total}} = \mathcal{L}_{\text{reconstruction}} + \beta \cdot \mathcal{L}_{\text{KL}}.$$

Here, β controls the trade-off between reconstruction fidelity and latent space regularization.

2.2.2 Convolutional Neural Network (CNN) with Residual Connections

The CNN model is designed to directly predict the reflection spectra from the input metasurface patterns by leveraging convolutional layers and residual connections [23]. The architecture effectively captures spatial hierarchies in the input patterns while mitigating gradient degradation through the use of skip connections.

The network begins with three 1D convolutional layers, each followed by ReLU activations. These layers progressively extract spatial features from the input patterns. Residual connections, implemented using 1×1 convolutions, allow the input of intermediate layers to bypass the transformations and directly contribute to the output. This mechanism preserves low-level features and facilitates more efficient gradient flow during backpropagation.

After the convolutional layers, the model applies max pooling [18] to reduce the feature dimensions. Fully connected layers then map the extracted features to

the desired output size (2×501), corresponding to the frequency-domain spectra for R_x and R_y.

The CNN model minimizes the MSE between the predicted and actual spectra, ensuring robust learning of the metasurface response.

2.3 Training and Evaluation

Both models were trained on the PLG and PLR datasets using the Adam optimizer. The datasets were split into training and testing subsets in an 80:20 ratio. During training, the models optimized their parameters to minimize prediction errors based on metrics such as MSE, Mean Absolute Error (MAE), and the R^2 score. These metrics evaluate the accuracy and robustness of the models in capturing the spectral response of metasurfaces.

To validate the models' performance, predicted spectra were compared with the actual spectra, and qualitative visualizations were generated to assess the fidelity of the predictions. The results demonstrate the capability of the models to efficiently predict the EM responses of complex metasurface designs.

3. Evaluation Metrics and Results

The performance of the Variational Autoencoder (VAE) and Convolutional Neural Network (CNN) models was evaluated using three standard error metrics: Mean Squared Error (MSE), Mean Absolute Error (MAE), and the coefficient of determination (R^2). These metrics provide a comprehensive assessment of the models' predictive accuracy and their ability to generalize over the PLG and PLR metasurface datasets.

The MSE is a widely used metric for regression tasks and measures the average squared difference between the predicted values and the ground truth. Formally, it is defined as:

$$\text{MSE} = \frac{1}{n}\sum_{i=1}^{n}(y_i - \hat{y}_i)^2,$$

where y_i and $\hat{y}_i$ denote the actual and predicted values, respectively, and n represents the total number of samples. MSE is particularly sensitive to larger errors, making it useful for highlighting significant deviations between predictions and ground truth.

In contrast, the MAE quantifies the average magnitude of prediction errors, irrespective of their direction. It is expressed as:

$$\text{MAE} = \frac{1}{n}\sum_{i=1}^{n}|y_i - \hat{y}_i|.$$

Unlike MSE, MAE is less sensitive to outliers and provides a more interpretable measure of the average error magnitude.

The R^2 score, or coefficient of determination, evaluates how well the model explains the variance in the target data. It is defined as:

$$R^2 = 1 - \frac{\sum_{i=1}^{n}(y_i - \hat{y}_i)^2}{\sum_{i=1}^{n}(y_i - \bar{y})^2},$$

where $\bar{y}$ is the mean of the actual values. An R^2 score close to 1 indicates that the model captures most of the variability in the data, whereas a negative R^2 suggests poor predictive performance.

These metrics were implemented using Python's `scikit-learn` library to ensure computational precision. Each metric provides unique insights into the models' performance. While MSE emphasizes the impact of large errors, MAE offers a straightforward interpretation of average deviation, and R^2 captures the proportion of variance explained by the model.

3.1 Performance Analysis

Table 1 summarizes the error metrics for the VAE and CNN models on the PLG and PLR datasets. The VAE consistently achieves lower MSE and MAE values and higher R^2 scores compared to the CNN, particularly on the PLG dataset, which features simpler polygonal structures. For the more complex PLR dataset, the VAE still outperforms the CNN, albeit with a smaller margin.

Model	**Metasurface**	**MSE**	**MAE**	**R^2**
VAE	PLG	1.5091	0.1639	0.8037
VAE	PLR	1.5907	0.2317	0.6001
CNN	PLG	1.7921	0.2111	0.7247
CNN	PLR	5.2395	0.3270	0.5432

TABLE 1. Performance metrics for VAE and CNN models on PLG and PLR metasurface datasets.

The results highlight significant differences in how the Variational Autoencoder (VAE) and Convolutional Neural Network (CNN) capture the spectral features of metasurfaces, particularly at resonance peaks where sharp variations dominate. As seen in Figure 2, the VAE closely follows the actual spectra for both x- and y-polarized components, successfully identifying resonance peaks and maintaining consistency across the frequency range. This consistency is especially noteworthy for x-polarized components, which often exhibit more abrupt resonance features due to their stronger dependence on geometric and material anisotropies of the metasurface. X-polarized components frequently interact more sensitively with edge effects, surface current distributions, and localized resonances, making them inherently more challenging to predict accurately. The VAE's latent space representation likely excels here because it leverages probabilistic modeling to capture a distribution over these complex spectral patterns, rather than relying solely on deterministic feature extraction. This approach enables the VAE to generalize better across a diverse dataset of metasurface designs, including those with intricate patterns like the Polygonal Rings, which are particularly sensitive to polarization effects.

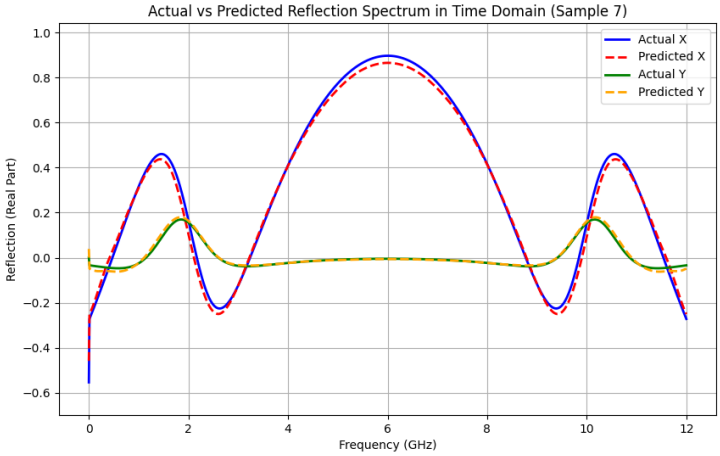

FIGURE 2. Actual vs Reconstructed Reflection Spectrum (Sample 7). The plot compares the actual and reconstructed reflection spectra for the x- and y-polarized components in the frequency domain, highlighting the VAE model's capability to accurately capture spectral features.

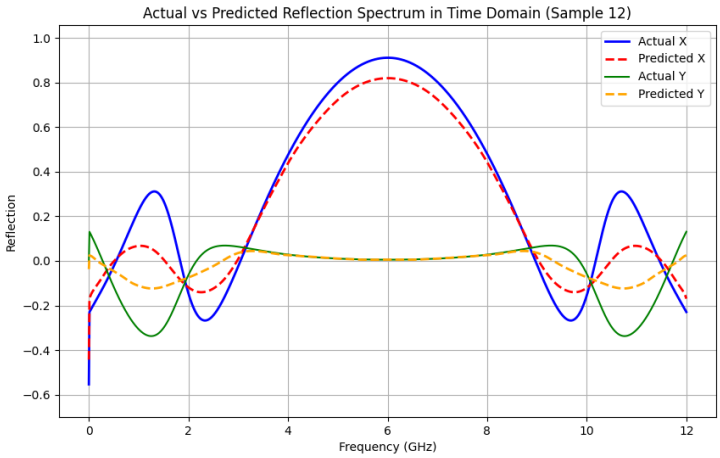

FIGURE 3. Actual vs Reconstructed Reflection Spectrum (Sample 7). The plot compares the actual and reconstructed reflection spectra for the x- and y-polarized components in the frequency domain, highlighting the CNN model's capability to accurately capture spectral features.

In contrast, the CNN predictions (Figure 3) show noticeable deviations from the actual spectra at critical resonance points. This is particularly evident for x-polarized components, where the CNN's reliance on spatial feature extraction without a mechanism for explicitly modeling spectral dependencies limits its ability to

resolve sharp variations. The smoothing effect observed in CNN predictions likely arises from its tendency to minimize error across the entire spectrum, which can lead to underestimation or overestimation of peak amplitudes at critical frequencies.

Evidence from other research supports our observations. Valleti et al. [24] demonstrated the superior performance of Variational Autoencoders (VAEs) in physics and chemistry datasets by effectively disentangling complex variability factors such as rotational and translational invariances in imaging data. Their study focused on atomic-scale imaging datasets, such as those derived from Scanning Transmission Electron Microscopy (STEM), which involve intricate spatial patterns, symmetry-breaking phenomena, and localized variations.

These challenges share similarities with our metasurface datasets, where intricate geometrical patterns dictate resonance behavior and sharp spectral features. In both cases, the datasets exhibit high-dimensional, non-linear dependencies that arise from the underlying physical structures. For metasurfaces, these dependencies are rooted in material anisotropies and edge effects that influence resonance peaks, while in the STEM data, they emerge from atomic-scale features, defects, and variations in crystalline arrangements.Their work underscores the relevance of VAEs in handling complex spectral features, directly aligning with the challenges in this study.

Notably, resonance peaks represent critical spectral features, as they govern the metasurface's electromagnetic behavior by dictating key properties such as phase, amplitude, and polarization control [25]. For x-polarized responses, these peaks often determine performance characteristics essential to applications like polarization sensitive filtering [26], beam steering [27], or sensing [28], where the control of sharp frequency-dependent features is paramount. The ability of the VAE to resolve these peaks highlights its potential for high-precision metasurface analysis.

3.2 Comparison with Related Work

The integration of deep learning in metasurface engineering has proven to be a powerful tool for addressing the computational challenges inherent in traditional simulation methods. Recent studies, such as An et al. [29], have demonstrated the utility of convolutional neural networks (CNNs) for modeling freeform dielectric metasurfaces, enabling rapid predictions of spectral responses across varying geometries. Their work, however, focuses on broad-spectrum responses without explicitly targeting polarized reflection spectra, as addressed in our study.

Similarly, Ghorbani et al. [30] developed a deep neural network (DNN)-based approach for the inverse design of metasurfaces under dual-polarized waves. While their work illustrates the potential of machine learning for metasurface optimization, the emphasis lies on generating metasurface patterns rather than predicting spectral responses. This differentiates their approach from ours, which directly predicts the x- and y-polarized reflection spectra of metasurfaces.

An et al. [31] further explored CNNs for accounting mutual coupling effects in metasurfaces. While their study enhances applications such as beam deflectors

and metalenses by considering inter-element interactions, it does not explicitly address predictive modeling of polarized responses. In contrast, our model leverages the frequency domain to effectively capture polarized spectral characteristics intrinsic to metasurfaces.

In comparison to these works, our study uniquely combines the use of VAEs and CNNs to predict polarized reflection spectra in the frequency domain. The integration of Fourier transforms allows our models to focus on the spectral characteristics of metasurfaces, resulting in enhanced accuracy and computational efficiency. This focus on polarized reflection spectra not only advances the predictive modeling of metasurfaces but also addresses practical applications in wireless communications and imaging, where polarization is a critical factor.

References

[1] O. Dănilă, A. Bărar, M. Vlădescu, and D. Mănăilă-Maximean. An extended k-surface framework for electromagnetic fields in artificial media. *Materials*, 14(24):7842, 2021.

[2] A. Bărar and O. Dănilă. Spectral Response and Wavefront Control of a C-Shaped Fractal Cadmium Telluride/Silicon Carbide Metasurface in the THz Bandgap. *Materials*, 15(17):5944, 2022.

[3] A. Bărar, S.A. Maclean, B.M. Gross, D. Mănăilă-Maximean, and O. Dănilă. Mixing Rules for Left-Handed Disordered Metamaterials: Effective-Medium and Dispersion Properties. *Nanomaterials*, 14(12):1056, 2024.

[4] Sean V Hum and Julien Perruisseau-Carrier. Reconfigurable reflectarrays and array lenses for dynamic antenna beam control: A review. *IEEE Transactions on Antennas and Propagation*, 62(1):183–198, 2014.

[5] Tie Jun Cui, Mei Qing Qi, Xue Feng Wan, Jian Zhao, and Qiang Cheng. Coding metamaterials, digital metamaterials, and programmable metamaterials. *Light: Science & Applications*, 3(10):e218, 2014.

[6] George V Eleftheriades and Keith G Balmain. Metamaterials: Enabling the design of novel antennas. *IEEE Antennas and Propagation Magazine*, 44(1):40–50, 2002.

[7] Aydogan Ozcan and Euan McLeod. Wide-field computational imaging using lens-free on-chip microscopy. *Trends in Biotechnology*, 35(11):1096–1110, 2017.

[8] Sean Molesky, Zibo Lin, Alexander Y Piggott, Wei Jin, Jelena Vuckovic, and Alejandro W Rodriguez. Inverse design in nanophotonics. *Nature Photonics*, 12(11):659–670, 2018.

[9] Hao Chen, Beibei Yang, Xianmin Zhang, and Xueying Zang. Review of the design and fabrication of metasurfaces for polarization control. *Nanophotonics*, 5(2):214–234, 2016.

[10] Jie Zhang, Lei Zhou, and Federico Capasso. Highly sensitive sensors using metasurfaces with phase singularities. *Advanced Materials*, 30(13):1704223, 2018.

[11] Cheng Chen, Zhao Fan, Changxi Zhang, Yujian Zheng, et al. Metasurface-enabled on-chip multiplexed diagnostics for detection of infectious diseases. *Nature Materials*, 19:973–982, 2020.

[12] Qiang Liang and Zhi Xu. Sensing beyond the diffraction limit with metasurfaces. *Nano Letters*, 19(2):1155–1162, 2019.

[13] O. Dănilă, D. Mănăilă-Maximean, A. Bărar, and V.A. Loiko. Non-layered gold-silicon and all-silicon frequency-selective metasurfaces for potential mid-infrared sensing applications. *Sensors*, 21(16):5600, 2021.

[14] O. Danila and D. Manaila-Maximean. Bifunctional metamaterials using spatial phase gradient architectures: Generalized reflection and refraction considerations. *Materials*, 14(9):2201, 2021.

[15] Allen Taflove and Susan C Hagness. *Computational Electrodynamics: The Finite-Difference Time-Domain Method*. Artech House, 2005.

[16] Fernando L Teixeira. Time-domain simulation of electromagnetic wave propagation using fdtd methods. *Electromagnetic Waves and Applications*, 22:743–757, 2008.

[17] Diederik P Kingma and Max Welling. Auto-encoding variational bayes. *arXiv preprint arXiv:1312.6114*, 2013.

[18] Yann LeCun, Léon Bottou, Yoshua Bengio, and Patrick Haffner. Gradient-based learning applied to document recognition. *Proceedings of the IEEE*, 86(11):2278–2324, 1998.

[19] Karim Achouri, Nima Chamanara, and Christophe Caloz. Computational analysis of metasurfaces. *IEEE Transactions on Antennas and Propagation*, 66(5):2580–2590, 2018.

[20] Anton Sturm, Weiliang Ma, Yingcheng Zhou, Shuyu Wang, Yue Liu, Jie Wu, Tie Jun Zhang, Lin Shi, Changchun Hao, Nicholas X. Fang, and Cheng-Wei Qiu. Sutd-prcm dataset and nas approach for complex metasurface design. *arXiv preprint arXiv:2203.00002*, 2022.

[21] Vinod Nair and Geoffrey E Hinton. Rectified linear units improve restricted Boltzmann machines. *Proceedings of the 27th International Conference on Machine Learning (ICML)*, pages 807–814, 2010.

[22] Nitish Srivastava, Geoffrey Hinton, Alex Krizhevsky, Ilya Sutskever, and Ruslan Salakhutdinov. Dropout: A simple way to prevent neural networks from overfitting. In *Journal of Machine Learning Research*, volume 15, pages 1929–1958, 2014.

[23] Kaiming He, Xiangyu Zhang, Shaoqing Ren, and Jian Sun. Deep residual learning for image recognition. In *Proceedings of the IEEE conference on computer vision and pattern recognition*, pages 770–778, 2016.

[24] M. Valleti, M. Ziatdinov, Y. Liu, and S.V. Kalinin. Physics and chemistry from parsimonious representations: image analysis via invariant variational autoencoders. *npj Computational Materials*, N/A(N/A):N/A, 2024.

[25] S. Abdollahramezani, O. Hemmatyar, H. Taghinejad, and W. Cai. Electrically driven reprogrammable phase-change metasurface reaching 80*Nature Communications*, 13:3746, 2022.

[26] Y. Cai, Y. Huang, K. Zhu, and H. Wu. Symmetric metasurface with dual band polarization-independent high-q resonances governed by symmetry-protected bic. *Optics Letters*, 46(16):4049–4052, 2021.

[27] K. Roy, R. Sinha, and C. Barde. Linear-to-linear polarization conversion using metasurface for x, ku, and k band applications. *Frequenz*, 76(5-6):303–311, 2022.

[28] E. Li, X.J. Li, B.C. Seet, A. Ghaffar, and A. Aneja. A metasurface-based ltc polarization converter with s-shaped split ring resonator structure for flexible applications. *Sensors*, 23(14):6268, 2023.

[29] S. An, B. Zheng, M. Y. Shalaginov, H. Tang, H. Li, L. Zhou, J. Ding, A. M. Agarwal, C. Rivero-Baleine, M. Kang, K. A. Richardson, T. Gu, J. Hu, C. Fowler, and H. Zhang. A freeform dielectric metasurface modeling approach based on deep neural networks. *arXiv preprint arXiv:2001.00121*, 2020.

[30] F. Ghorbani, J. Shabanpour, S. Beyraghi, H. Soleimani, H. Oraizi, and M. Soleimani. A deep learning approach for inverse design of the metasurface for dual-polarized waves. *Applied Physics A*, 127:869, 2021.

[31] S. An, B. Zheng, M. Y. Shalaginov, H. Tang, H. Li, L. Zhou, Y. Dong, M. Haerinia, A. M. Agarwal, C. Rivero-Baleine, M. Kang, K. A. Richardson, T. Gu, J. Hu, C. Fowler, and H. Zhang. Deep convolutional neural networks to predict mutual coupling effects in metasurfaces. *arXiv preprint arXiv:2102.01761*, 2021.